Earthquakes and Structures, *Vol. 19, No. 2 (2020) 145-156*
DOI: https://doi.org/10.12989/eas.2020.19.2.145

24 January 2020 Sivrice (Elazığ) earthquake damages and determination of earthquake parameters in the region

Ercan Işık[1a], Mehmet Cihan Aydın[1b] and Aydın Büyüksaraç[*2]

[1]Department of Civil Engineering, Faculty of Engineering and Architecture, Bitlis Eren University, TR-13100, Bitlis, Turkey
[2]Çan Vocational School, Çanakkale Onsekizmart University, TR-17100, Çanakkale-Turkey

(Received March 24, 2020, Revised August 9, 2020, Accepted August 11, 2020)

Abstract. The 24 January 2020 (Mw=6.8) earthquake with epicentre in Elazığ (Sivrice) on the East Anatolian Fault Zone caused loss of life and property. The information was given about the seismotectonic setting and regional seismicity along this fault zone and aftershock activity and ground motion data of this earthquake. Earthquake parameters were obtained for five different earthquake stations which were closer to the epicentre. Horizontal and vertical design spectra were obtained for the geographic locations for each earthquake station. The obtained spectra for the earthquake epicentre were compared with selected appropriate attenuation relationships. The damages after earthquake were evaluated via geotechnical and structural aspects. This study also aims to investigate the cause-effect relationships between structural damage in reinforced-concrete and masonry structures, respectively. The lack of engineering services was effective on the amount of damage in masonry structures. Insufficient reinforcement and concrete strength, dimensions and inadequate detailing increased the amount of damage in reinforced-concrete structures. Importance should be given to negative parameters that may weaken the defence mechanisms of structures for earthquake-resistant structural design.

Keywords: Sivrice; earthquake; masonry; reinforced-concrete; structural damages; spectra

1. Introduction

Significant loss of life and property forming after every earthquake brings to the agenda the importance of studies about this topic and precautions which should be taken. In this context, identification of any damage occurring after an earthquake and determination of the seismicity features of a region are encountered as an inseparable part of modern natural disaster management. Assessing and managing all this information together is important for spatial planning and urban renewal (İnel *et al*. 2013, Rafi *et al*. 2015, Işık *et al*. 2017, Hadzima and Nyarko *et al*. 2018, Işık 2016, Spos and Hadzima and Nyarko 2017, Kabeyasawa 2017, Taşkın and Tugsal 2011, Karababa and Pomonis 2011). Finally, the earthquake occurring in Sivrice in the east of Turkey is the latest example of this.

When the tectonic processes involving Turkey are considered, a very complex system is revealed. Dominant characteristic movements within this complexity reveal the description of tectonism in Turkey. Plate movements are examined during explanations of tectonism and the most common method is to observe plate movements. Currently plate movements are most effectively observed and measured with GPS. From GPS data, both plate movement rates and directions can be obtained. The Anatolian block is basically affected by two important plate movements. The first and most effective of these is motion linked to anticlockwise rotation of the African plate and northward pushing of the Arabian plate. This collision event pushes the southeast of the Anatolian plate northward. The other significant movement is better known as the clockwise motion of the Eurasian plate. The effect of this movement is to push the Anatolian block southward. As a result, the Anatolian block is affected by two significant compressions and displacement is towards the west-southwest. These effects observed in the Anatolian block are seen in the form of shearing between Erzincan-Karlıova and the stress occurring with the effect of this motion occasionally leads to earthquakes due to fracturing. The dominant fracture system in the Anatolian block, containing many faults, is the North and East Anatolian Fault Zones. Additionally, another fracture region is the Northeast Anatolian Fault Zone (NAFZ) extending northeast from Karlıova. Thus, Karlıova acts like a triple junction fracture zone. Due to the southeast-oriented motion of the west of the Anatolian block, Western Anatolia is expanding towards the south in the south and toward the north in the north (Fig. 1).

The East Anatolian region is one of the regions where seismic activity is most intensely experienced. Especially Karlıova, a county linked to Bingol, is equivalent to the junction of the NAFZ and the East Anatolian Fault zones (EAFZ). These two faults with intercontinental transform fault characteristics bound the Anatolian plate and the area where a cross fault system has developed between these two is the region with longest active fault length in Turkey. The

*Corresponding author, Ph.D. Professor
E-mail: absarac@comu.edu.tr
[a] Ph.D. Assosiate Professor
E-mail: eisik@beu.edu.tr
[b]Ph.D. Professor
E-mail: mcaydin@beu.edu.tr

http://www.techno-press.com/journals/was&subpage=7
ISSN: 2092-7614 (Print), 2092-7622 (Online)

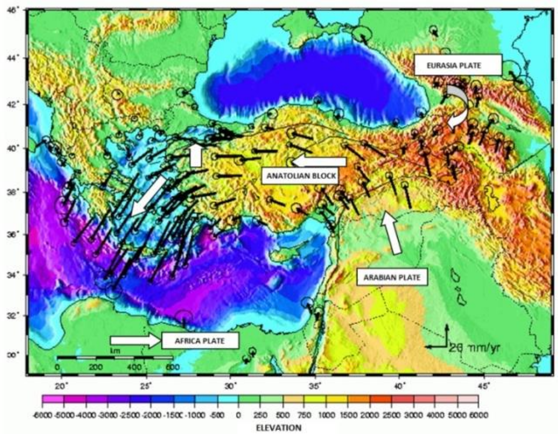

Fig. 1 Tectonic system including the Anatolian Block (adapted from McClusky *et al*. 2000)

dominant fault mechanisms in the region comprise the Bitlis Suture Zone, NAFZ and EAFZ. Located within this region, the Mw=6.8 earthquake occurring on 24 January 2020 in Elazığ (Sivrice) attracted attention to the EAFZ. The EAFZ is Turkey's second most important fault zone in terms of causing loss of life and property. The 24 January 2020 Sivrice (Elazığ) Earthquake (Mw=6.8) provides valuable information on refractive behavior as it is the largest earthquake to have occurred along the Eastern Anatolian Fault Zone (EAFZ) for more than a century (Pousse-Beltran *et al*. 2020). The source of many large earthquakes in the historical period, the EAFZ entered a very active period in the 19th century. The earthquake series began with the Antakya earthquake in 1822, continued with earthquakes in 1866, 1872, 1874, 1875, and 1893, and finally the 1905 Malatya earthquake. After this earthquake, there was a relatively calm period with no earthquake large enough to produce surface ruptures. This calmness was stated to be temporary and significant stress accumulated. The Sivrice earthquake broke this silence and brought to the agenda the question of whether a new earthquake series will occur. The Sivrice earthquake was felt in many settlement areas. In the region with many aftershocks after the main shock, this earthquake entered the list of significant earthquakes in the EAFZ due to loss of life, injuries, structural damage and economic losses. The greatest structural damage occurred in settlement areas in Elazığ and Malatya.

It is important to determine the cause-effect relationships for the damages after the earthquake. In this context, the geotechnical and structural damages caused by the Sivrice earthquake were investigated. It has been observed that the negative features of structures have caused an increase in damage extent because of the weakening the structural defence mechanisms. Information about the negative structural features commonly encountered in Sivrice earthquake was given in this study. Additionally, earthquake parameters for the earthquake epicentre are calculated for the best and worst situations in relation to local soil conditions. Earthquake parameters were calculated for the geographic locations of five different earthquake stations located closest to the epicentre. Horizontal and vertical design spectra curves were obtained

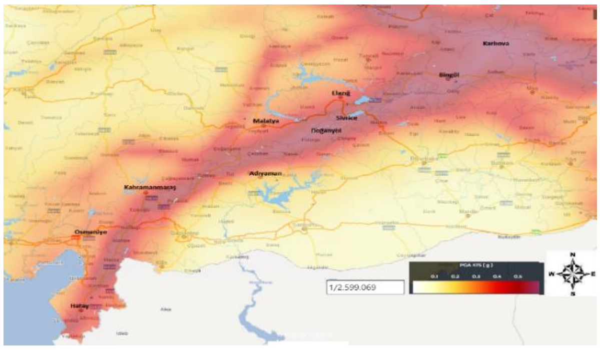

Fig. 2 EAFZ and affected settlements (adapted from https://tdth.afad.gov.tr)

for the DD-2 earthquake ground motion level for an earthquake with 10% annual probability of exceedance (recurrence period 475 years) for all stations. The obtained spectra for the earthquake epicentre were compared with selected appropriate attenuation relationships. Interpretations were made for the geotechnical damages observed in the field were made. Masonry and reinforced-concrete (RC) structures are examined in terms of structural damages, separately. The cause and effect relationships of the damages were evaluated within the framework of earthquake resistant building design.

2. East Anatolian Fault Zone (*EAFZ*)

Attracting attention after the Sivrice earthquake, the EAFZ separates the Arabian plate from the Anatolian plate, is the left-lateral conjugate of the NAFZ and is a left-lateral strike-slip fault with NE-SW strike. It joins with the Dead Sea Fault near Türkoğlu and with the NAFZ near Karlıova. The zone comprising many left-lateral strike-slip faults with differing features between Karlıova-Antakya is called the EAFZ (Arpat and Şaroğlu 1972). The EAFZ was assessed as comprising many segments by different researchers. Şaroğlu *et al*. (1992a) stated the fault was separated into six segments based on surface fault traces. Hempton *et al*. (1981) separated the fault into five segments based on geometry and strike changes. Barka and Kadinsky-Cade (1988) separated 14 segments according to geometric discontinuities, surface ruptures and seismicity features. Duman and Emre (2013) separated the EAFZ into five segments based on similar reasoning. These faults were stated to be the Karlıova-Bingöl, Palu-Hazar, Hazar Lake-Sincik, Çelikhan-Erçenek, Gölbaşı-Türkoğlu and Türkoğlu-Antakya segments. Further south, the Syria-Lazkiye earthquakes are included in this zone. The EAFZ has nearly 30 km width, with nearly 700 km length (Haktanır and Elcüman 2007, Aksoy *et al*. 2007). The closest settlement areas to this fault zone are Hatay, Osmaniye, Kahramanmaraş, Adıyaman, Malatya, Elazığ, Bingöl and related centres. The location of these settlement areas on the map is shown in Fig. 2.

Significant historical and instrumental period earthquakes on the EAFZ were shown in Table 1. Here, earthquakes are grouped as historical and instrumental

Table 1 Earthquakes on the EAFZ (AFAD 2020, Calvi 1941, Biricik and Korkmaz 2001, Köküm and Özçelik 2020, Sançar and Akyüz 2014, Sunkar 2018, KOERI 2020, Anonymous-3 2020, Anonymous-4 2020)

No	Date	Region	Intensity	Magnitude
		Historical Period		
1	148 BC	Antakya	VIII	
2	69 BC	Antakya	IX	
3	37 BC	Antakya	VIII	
4	AD 53	Lazkiye-Antakya	VIII	
5	396	Antakya	VIII	
6	526	Antakya	IX	
7	529	Antakya	IX	
8	1544	Elbistan	VIII	
9	1568	Lazkiye	VIII	Ms=6.0
10	1626	Halep	IX	Ms=7.3
11	1738	Amik Lake (Hatay)	VIII	Ms=6.2
12	1789	Elazığ	VIII	
13	1796	Lazkiye	VIII-IX	Ms=6.8
14	1822	Antakya	IX	Ms=7.0
15	1866	Karlıova (Bingöl)		Ms=6.8
16	1872	Amik Lake (Hatay)	VIII-IX	Ms=7.2
17	1874	Elazığ	IX	Ms=7.1
18	1875	Elazığ	VI	Ms=6.7
19	1875	Palu		Ms=6.1
20	1893	Malatya	IX	
		Instrumental Period		
1	04 Dec 1905	Pütürge (Malatya)		Ms=6.8
2	20 Mar 1945	Ceyhan (Adana)		Ms=6.0
3	22 Oct 1952	Misis (Adana)		Ms=5.6
4	14 June 1964	Sincik (Adıyaman)		Ms=6.0
5	22 May 1971	Bingöl		Ms=6.8
6	06 Sep1975	Lice (Diyarbakır)		M=6.6
7	1979	Adana-Kozan		Ms=5.1
8	5 May 1986	Sürgü (Malatya)		Mw=6.0
9	1986	Gaziantep		Ms=5.0
10	1991	Kadirli (Adana)		Ms=5.2
11	1994	Ceyhan (Adana)		Ms=5.0
12	22 Jan 1997	Samandağ (Hatay)		Mw=5.7
13	27 June 1998	Yüreğir (Adana)		Mw=6.2
14	01 May 2003	Bingöl		Mw=6.3
15	11 Aug2004	Sivrice –Elazığ		Mw=5.6
16	09 Feb 2007	Sivrice (Elazığ)		Mw=5.5
17	21 Feb 2007	Sivrice (Elazığ)		Mw=5.7
18	08 Mar2010	Kovancılar (Elazığ)		Mw=6.1

period earthquakes. According to both historical and instrumental period earthquakes, the central and northeast sections of the EAFZ appear to have more intense activity. Contrary to this, it is understood that no destructive earthquake occurred on the Gölbaşı-Türkoğlu segment, especially, in the last 500-year period (Kartal and Kadiroğlu 2013).

3. Sivrice (*Elazığ*) earthquake (*Mw=6.8*)

The depth of the earthquake occurring on 24.01.2020 was determined as 8.06 km. After the main shock, 995

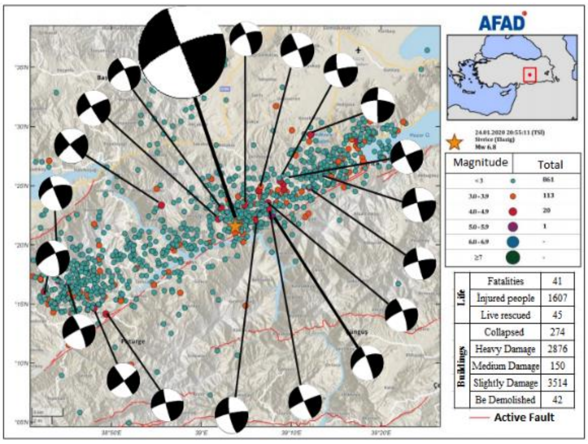

Fig. 3 Main shock of the Sivrice earthquake and aftershock activity (adapted from AFAD 2020, Anonymous-1 2020, Anonymous-2 2020)

Table 2 Accelerometer stations in the region and measured acceleration values (AFAD 2020, Anonymous-1 2020)

Station	N-S (gal)	E-W (gal)	Vertical (gal)	Distance (km)R_{epi}
Sivrice/Elazığ	237.99	292.77	190.09	24
Pötürge/Malatya	206.91	239.24	153.87	25
Gerger/Adıyaman	94.03	110.11	60.75	37
Centre/Elazığ	119.28	140.73	66.31	36
Maden/Elazığ	26.29	33.97	22.78	53

aftershocks with magnitude varying from 0.8 to 5.1 were recorded up to 12:25 on 27.01.2020 (Fig. 3). The clear duration of the earthquake was calculated as 20.4 s according to initial determinations. When focal mechanism solutions after the earthquake are assessed together, the Mw=6.8 earthquake developed on the Sivrice-Pötürge segment of the left-lateral strike-slip EAFZ and it is thought rupture developed in a 50-55 km area (AFAD2020). The earthquake was felt mainly in Elazığ province and its districts and in the East Anatolia, Southeast Anatolia, Central Anatolia and Black Sea regions (KOERI 2020, Anonymous-1 2020).

The acceleration values measured at five stations located closest to the earthquake epicenter are given in Table2 (Anonymous-5 2020).

With the Turkish Seismic Design Code entering force on 1 January 2019 (TSDC-2018) and the entry into use of the Turkish Earthquake Hazard Map, the earthquake parameter values for the earthquake epicenter were obtained by the aid of the Turkish Earthquake Hazard Map Interactive Web Application (TSDC-2018, https://tdth.afad.gov.tr). The seismic risk map used in the interactive web application is shown in Fig. 4 (Anonymous-2 2020).

The TSDC-2018 represents earthquake ground motion level in four different ways, different to previous codes. The earthquake ground motion levels used within the scope of the study are given in Table 3.

The peak ground acceleration (PGA) and peak ground velocity (PGV) values obtained for different probabilities of exceedance in 50 years for the nearest accelerometer stations are shown in Table 4.

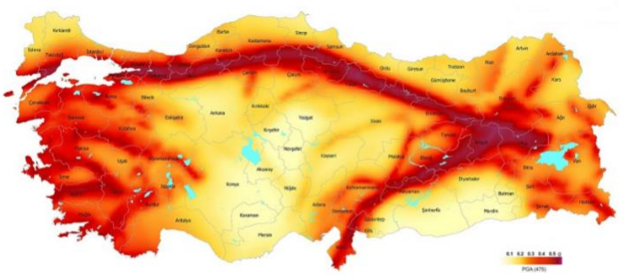

Fig. 4 Seismic risk map for Turkey (http://tdth.afad.gov.tr)

Table 3 Earthquake ground motion levels (TSDC-2018, Anonymous-2 2020)

Earthquake level	Return period (years)	Probability of exceedance (in 50 years)	Description
DD-1	2475	0.02	Largest earthquake ground motion
DD-2	475	0.1	Standard design earthquake ground motion
DD-3	72	0.5	Frequent earthquake ground motion
DD-4	43	0.68	Service earthquake motion

Table 4 PGA and PGV values for different probabilities of exceedance in 50 years for accelerometer stations

Location	Peak Ground Acceleration (g)			
	Probability of Exceedance in 50 Years			
	2%	10%	50%	68%
Elâzığ/Sivrice	1.101	0.622	0.230	0.145
Malatya/Pötürge	1.145	0.651	0.237	0.144
Adıyaman/Gerger	0.683	0.371	0.149	0.106
Elazığ /Centre	0.711	0.383	0.148	0.099
Elazığ /Maden	0.878	0.478	0.185	0.127
Location	Peak Ground Velocity (cm/s)-PGV			
	Probability of Exceedance in 50 Years			
	2%	10%	50%	68%
Elâzığ/Sivrice	82.292	44.036	12.853	7.463
Malatya/Pötürge	81.004	45.022	12.718	7.018
Adıyaman/Gerger	41.535	21.735	8.116	5.535
Elazığ /Centre	45.903	23.920	8.922	5.854
Elazığ /Maden	54.881	28.570	10.247	6.670

Short period map spectral acceleration coefficient (S_S) and map spectral acceleration coefficient for the period of 1.0 seconds (S_1) for the nearest accelerometer stations was given in Table 5.

The coordinates of the earthquake epicenter were determined as 38.3593 and 39.0630 (AFAD 2020). This geometric location is shown on the EAFZ and on the satellite image in Fig. 5.

ZA and ZE local soil class types were selected to obtain the largest and smallest earthquake parameter values for the Sivrice earthquake according to updated Turkish Earthquake Hazard Map. S_S, S_1, PGA, PGV, local ground effect coefficients (F_S and F_1), design spectral acceleration coefficients (short period design spectral acceleration coefficient (S_{DS}), design spectral acceleration coefficients

Table 5 S_S, S_1 values for different probabilitie of exceedance in 50 years for accelerometer stations

Location	Short period map spectral acceleration coefficient (S_S)			
	Probability of Exceedance in 50 Years			
	2%	10%	50%	68%
Elâzığ/Sivrice	2.762	1.504	0.539	0.330
Malatya/Pötürge	2.868	1.578	0.548	0.329
Adıyaman/Gerger	1.701	0.883	0.344	0.243
Elazığ /Centre	1.734	0.912	0.342	0.228
Elazığ /Maden	2.185	1.148	0.428	0.296
Location	Map spectral acceleration coefficient for the period of 1.0 seconds (S_1)			
	Probability of Exceedance in 50 Years			
	2%	10%	50%	68%
Elâzığ/Sivrice	0.778	0.396	0.126	0.075
Malatya/Pötürge	0.782	0.403	0.122	0.069
Adıyaman/Gerger	0.446	0.233	0.085	0.057
Elazığ /Centre	0.496	0.257	0.097	0.063
Elazığ /Maden	0.601	0.306	0.107	0.069

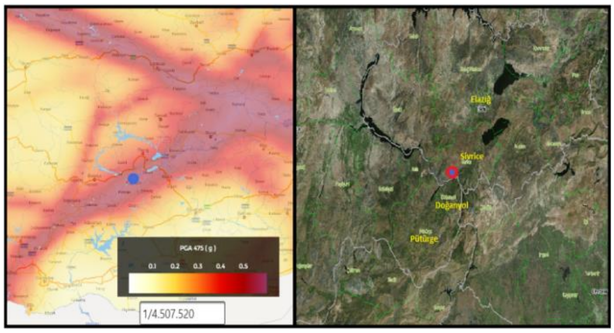

Fig. 5 Fault and field appearance of earthquake epicenter (adapted from https://tdth.afad.gov.tr)

Table 6 Comparison of earthquake parameters for earthquake epicenter (Anonymous-2 2020)

	ZA				ZE			
	DD-1	DD-2	DD-3	DD-4	DD-1	DD-2	DD-3	DD-4
S_S	2.913	1.604	0.578	0.339	2.913	1.604	0.578	0.339
S_1	0.819	0.419	0.132	0.074	0.819	0.419	0.132	0.074
PGA	1.165	0.665	0.250	0.149	1.165	0.665	0.250	0.149
PGV	94.26	52.21	13.77	7.456	94.27	52.21	13.77	7.456
F_S	0.800	0.800	0.800	0.800	0.800	0.800	1.575	2.151
F_1	0.800	0.800	0.800	0.800	2.000	2.362	3.912	4.200
S_{DS}	2.330	1.283	0.462	0.271	2.330	1.283	0.910	0.729
S_{D1}	0.655	0.335	0.106	0.059	1.638	0.990	0.516	0.311
T_A	0.056	0.052	0.046	0.044	0.141	0.154	0.113	0.085
T_B	0.281	0.261	0.228	0.218	0.703	0.771	0.567	0.426
T_{AD}	0.019	0.017	0.015	0.015	0.047	0.051	0.038	0.028
T_{BD}	0.094	0.087	0.076	0.073	0.234	0.257	0.189	0.142

for 1.0 second period (S_{D1}), horizontal and vertical elastic design spectra were obtained from the web application for the earthquake epicentre by using different earthquake ground motion levels for the selected local soil class types were shown in Table 6. Horizontal elastic design acceleration spectrum corner period (T_A and T_B), vertical elastic design acceleration spectrum corner period (T_{AD} and

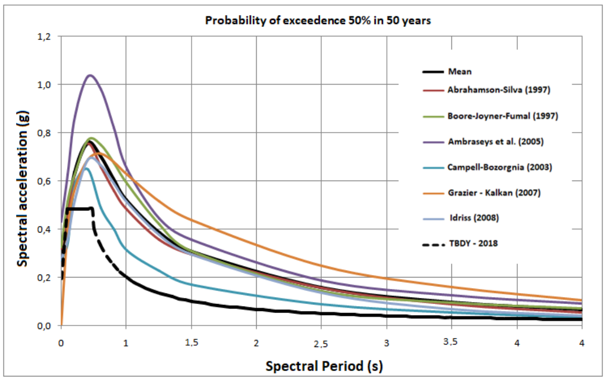

Fig. 6 Comparison of spectral responses for the return period of 72 years in Sivrice

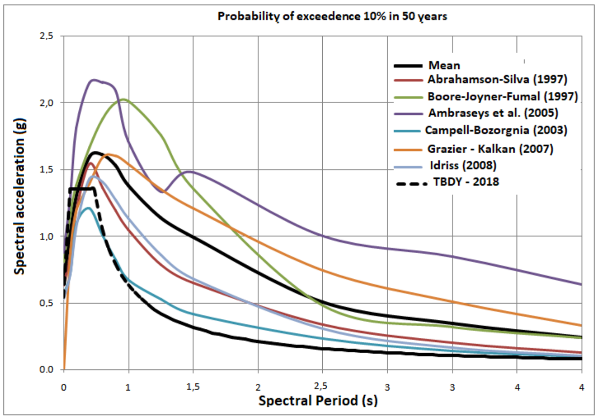

Fig. 7 Comparison of spectral responses for the return period of 475 years in Sivrice

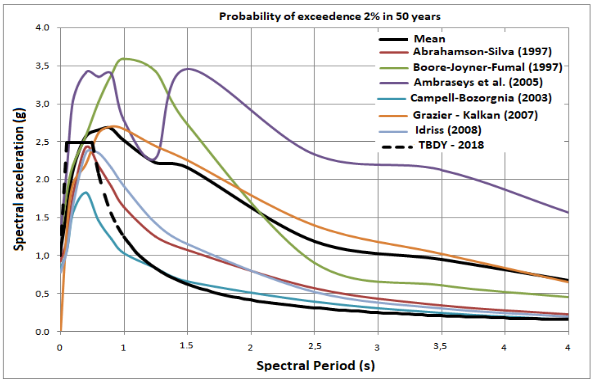

Fig. 8 Comparison of spectral responses for the return period of 2475 years in Sivrice

T_{BD}) were also obtained through the same application for the earthquake epicentre.

In this study, six worldwide applicable empirical attenuation relationships are used to compare the spectra obtained for the Sivrice earthquake epicentre. Abrahamson-Silva (1997), Boore-Joyner-Fumal (1997), Ambraseys *et al.* (2005), Campell and Bozorgnia (2003), Grazier-Kalkan (2007) and Idriss (2008) are the selected attenuation relationships in this study. The comparison of the response spectra for 50% probability to be exceeded in 50 years and a return period of 72 years for earthquake epicentre was shown in Fig. 6.

The comparison of the response spectra for 10% probability to be exceeded in 50 years and a return period of 475 years for Sivrice was shown in Figure 7.

The comparison of the response spectra for 2% probability to be exceeded in 50 years and a return period of 2475 years for Sivrice was shown in Fig. 8.

The study additionally performed calculations for the nearest earthquake stations. The locations of these earthquake stations were shown on Fig. 9.

Comparisons of the earthquake parameters obtained for the station locations are shown in Table 7. The earthquake

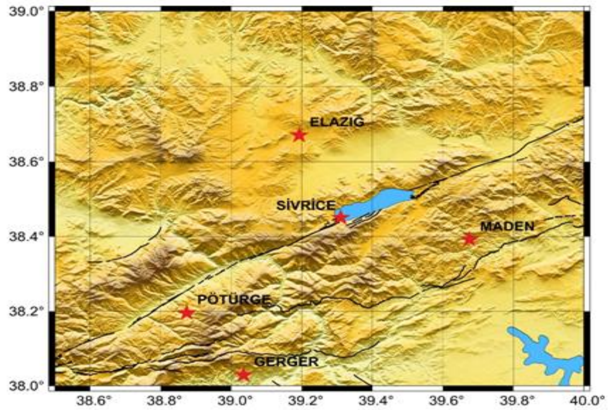

Fig. 9 Nearest earthquake station locations

Table 7 Comparison of earthquake parameter values

Parameter	County/Province				
	Sivrice / Elâzığ	Pötürge / Malatya	Gerger / Adıyaman	Centre / Elazığ	Maden / Elazığ
S_S	1.504	1.578	0.883	0.912	1.148
S_1	0.396	0.403	0.233	0.257	0.306
PGA	0.622	0.651	0.371	0.383	0.478
PGV	44.036	45.022	21.735	23.920	28.570
F_S	0.800	0.800	1.194	1.170	0.982
F_1	2.416	2.394	3.135	3.015	2.776
S_{DS}	1.203	1.262	1.054	1.067	1.127
S_{D1}	0.957	0.965	0.730	0.775	0.849
T_A	0.159	0.153	0.139	0.145	0.151
T_B	0.795	0.764	0.693	0.726	0.754
T_{AD}	0.053	0.051	0.046	0.048	0.050
T_{BD}	0.265	0.255	0.231	0.242	0.251

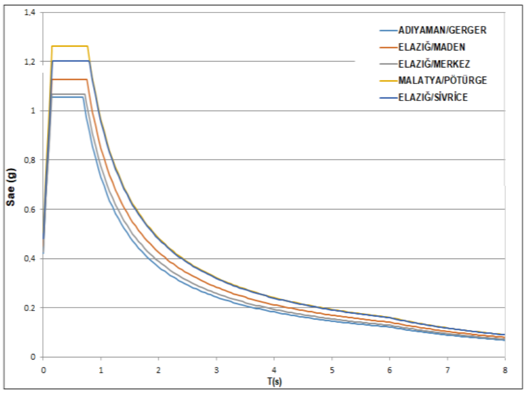

Fig. 10 Comparison of horizontal design spectra obtained for different stations with 10% probability of exceedance 50 years

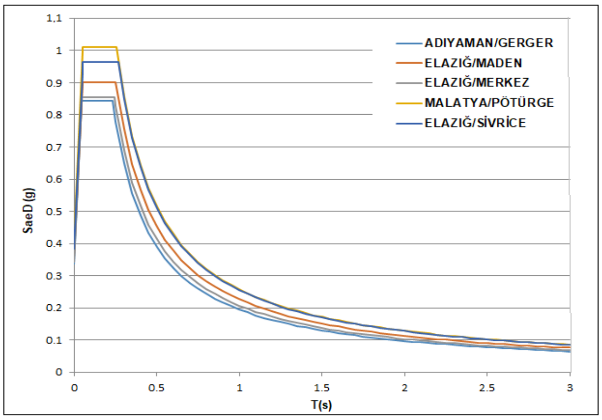

Fig. 11 Comparison of vertical design spectra obtained for different stations with 10% probability of exceedance 50 years

Fig. 12 Ground rupture observed after the earthquake

ground motion level DD-2 for an earthquake with 10% probability of exceedance 50 years (recurrence period 475 years) and the ZE class as the worst local ground class were noted.

The comparison of horizontal design spectra obtained separately according to ground motion level for DD-2 earthquake at the points for each of the five earthquake stations was shown in Fig. 10. The comparison of the obtained vertical design spectra was shown in Fig. 11.

4. Geotechnical damages after Sivrice earthquake

In addition to structural damage, earthquakes cause damage to the earth's surface. Earthquakes cause dangerous outcomes like landslides increasing losses in the second-degree. Ground damage was commonly observed in Çevrimtaş village, 0.81 km from the earthquake epicentre, and Doğanbağı village, 1.38 km from the epicentre and destroyed by the earthquake. Ruptures were formed in the field and progressed with a definite traceable strike. Fractures and rock fall events were observed on roads in this region. Visual images of these damages were shown in Fig. 12.

On the other hand, local liquefaction was observed on the shore of Lake Hazar. However, the fact that liquefaction is at a very low level and not seen in any other area means that this earthquake does not create an acceleration value that exceeds the threshold acceleration value (Fig. 13)

Fig. 13 Local liquefaction traces observed on the shore of Lake Hazar

5. Damage observed in Masonry Structures

Masonry structures have been built since the beginning of humanity and generally do not involve any engineering services, are constructed by local experts and laborers from local material and continue to be commonly used in rural areas. The strength of these types of structure to earthquake behavior is very low. Due to the lack of application of earthquake-resistant structural design rules in rural areas affected by the Sivrice earthquake, significant damage was caused to masonry structures. Masonry structures in this region generally use stone or mudbrick with earth or rarely cement mortar used to adhere the structure. Earthen roofs supported by wooden beams form the roof.

In masonry structures, the load-bearing system comprises vertical walls made of different material like

Fig. 14 Completely collapsed masonry structures

Fig. 15 Damage observed in masonry structures (a) separation at corners, (b) damage to structural wall, (c) damage to non-structural elements, (d) damage caused by large openings, (e) structural wall damage caused by large window opening, (f) out-of-plane damage to structural wall, (g) out-of-plane damage to structural wall, (h) damage to structural wall by large window openings, (i) earthen roof damage, damage to wooden beams and out-of-plane damage

bricks and natural stones. Additionally, most traditional and historical structures are constructed of masonry. The reason for choosing masonry structures is that they can be easily made of local material and are economic. These types of structures are generally constructed haphazardly without sufficient engineering knowledge or awareness of standards. As masonry structures consist of loose material like bricks and mortar, they have low ductility. Additionally, they have lower capacity to absorb earthquake energy compared to RC structures. The walls of masonry structures both surround the area of use in the building and act as load-bearing elements. Load transfer is between the material used and the mortar. The elements of the load-bearing system in masonry buildings comprise floors, the walls where they are supported and the foundations of these walls. Damage to masonry structures generally forms as cracks in walls, settling of foundations, and disruption or displacement of material used. Generally, the tensile strength of wall material used in masonry structures and the shear strength of mortar are low. The most important cause of damage is shear strain forming in the walls because of the earthquake causing fractures, separations and displacement due to tensile strain. Additionally, adherence must be provided between material to ensure healthy load transfer (Bilgin and Huta 2018, Çırak 2011, Karaşin *et al*. 2016, Karaşin and Öncü 2009, Korkmaz *et al*. 2016, Hadzima and Nyarko *et al*. 2018b, Özlük *et al*. 2019, Özlük *et al*. 2019, Bilgin and Hysenlliu 2020). Within the scope of this study, the structures in two settlements closest to the epicenter of the Sivrice earthquake of Çevrimtaş and Doğanbağı villages were primarily examined. Fig. 14 shows fully collapsed masonry structures.

Fig. 15 shows images of different types of damage commonly observed in masonry structures constructed using local material.

Fig. 16 Damage by poor concrete properties

Fig. 17 Improper detailing transverse reinforcement (90˚ instead of 135˚)

Fig. 18 Insufficient detailing and corrosion of reinforcement

6. Damages observed in Reinforced-Concrete (RC) structures

Material strength in RC structures directly affects the behavior of the structure under the effect of earthquakes (Işık and Özdemir 2017). Concrete obtained by passing through many stages, lack of use of necessary engineering information in these stages and lack of enough care is the weak point of RC. Damage is primarily associated with concrete strength. Low and poor features of concrete have increased degree of damage in RC buildings. This was clearly determined based on observations after the Sivrice

Fig. 19 Damage to non-structural elements, (a) chimney damage, (b)roof gable wall damage, (c)damage to external cladding, (d) stair damage

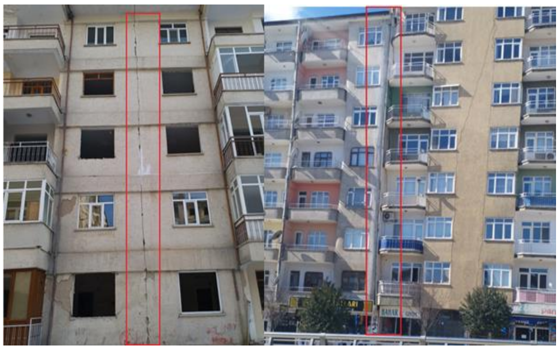

Fig. 20 Separation damage to adjacent buildings without dilatation joints

earthquake. Inappropriate grain distribution and size in aggregate, direct use of aggregate obtained from rivers found in the region and inappropriate concrete compression processes led to concrete with very low strength to segregation. Visual images of low strength concrete are shown in Fig. 16.

While transverse reinforcement used in structural elements in buildings that built in earthquake regions should have 135°, they were bent at 90°. Visual images related to this situation are shown in Fig. 17. Additionally, the lack of use of crossties negatively affected the degree of damage.

One of the damages observed in damaged structures was insufficient concrete cover layers, removing the adherence between the reinforcement and concrete. This situation also caused corrosion of reinforcement. Reinforcement corrosion was commonly observed due to the content of the aggregate used in the concrete mix. Insufficient fixtures and corrosion are shown in Fig. 18. Corrosion of reinforcement for different reasons reduces the load-bearing capacity.

Damage was observed in non-structural elements also. Damage was observed in roof gable walls, ventilation chimneys, external cladding and stairs. Damage to these elements was shown in Fig. 19.

Though significant structural damage was not observed in relation to not leaving necessary dilatation spaces between adjacent buildings, the expected separation between buildings was observed (Fig. 20).

The lack of enough transverse reinforcement caused a variety of damage to structural elements. The clearest form of this damage was buckling of reinforcement longitudinally.

Fig. 21 Insufficient transverse reinforcement intervals and damage

Fig. 22 Different infill wall damages

Fig. 23 Damage due to overhangs in structures

Fig. 24 Different design defects, (a) insufficient and smooth reinforcement use, (b) insufficient reinforcement, (c) column-beam eccentricity, (d) insufficient reinfor-cement where column-beams joint and beams with inappropriate size, (e) Insufficient beam size, (f) stud beam, (g) shear crack on column, (h) no overlap in beam-column joint

Buckling of longitudinal reinforcement caused direct damage to concrete leading to loss of load-bearing capacity of structural elements. Additionally, improper detailing transverse reinforcement in columns was observed. Visual images related to insufficient transverse reinforcement intervals and damage to columns and beams are shown in Fig. 21.

Infill walls are used to fill the frames in RC structures. At the same time, they limit the movement of the frame contributing to horizontal load carrying. Damage beginning with separations between infill walls and frames later proceeded to cross fractures with X form with higher horizontal load levels in earthquakes. Infill wall damage was commonly observed after the Sivrice (Elazığ) earthquake. This damage was observed as cross fractures, wall separations, frame-wall separations and space wall damage in many buildings. Separation damage in walls (Fig. 22(a), 22(j)), frame-wall separation (Figs. 22(b) and 22(h)), X form cross fractures (Figs. 22(c), 22(d), 22(f), 22(i) and 22(l)) and damage in wall spaces (Figs. 22(e) and 22(k)) are shown below.

Damage of varying types occurred due to overhangs in structures. Design of structures without overhangs is one of the solutions that can be applied to prevent this type of damage. Damage due to overhang is shown in Fig. 23.

In addition to this damage, various types of damage formed in structural elements built without abiding by the rules of earthquake-resistant structural design. This damage is notable including design defencies such as shear damage in columns, insufficient longitudinal reinforcement, use of smooth reinforcement, insufficient reinforcement dimensions, stud beams at connections of beams within the load-bearing system, insufficient reinforcement in beam-column regions and eccentricity of column-beam connections. Images related to these design defencies are shown in Fig. 24.

7. Conclusions

The 24 January 2020 Sivrice (Elazığ) earthquake occurred as an expected earthquake in the region. The earthquake that occurred correspond in position to the 1874 (Mw = 7.1) and 1875 (Mw = 6.7) earthquakes. In particular, the lower end of the 1874 segment and the location of the 1875 segment are almost at the same location. In this sense, the earthquake that occurred on January 24, 2020 is in an unexpected location in terms of location. The largest acceleration measured for this earthquake was 0.293 g at the Elazığ (Sivrice) earthquake station. The predicted PGA values for Elazığ province and counties according to 2007 earthquake regulations were stated to be between 0.3g and 0.4g. This value may show differences according to a geometric location and includes regionally variable values. The Turkish Earthquake Hazard Map began to be used with the entry into force of the 2019 earthquake regulations. This map began to perform special calculations for each geographical location. Using this map, earthquake parameters were calculated for the earthquake epicentre and the locations of five different earthquake stations. PGA was calculated as1.165 g for the largest earthquake ground motion, 0.665 g for the standard design earthquake ground motion and 0.250 g for frequent earthquake ground motion for the Sivrice earthquake epicentre. Additionally, calculations based on the standard design earthquake ground motion (DD2) for the geographic locations of the five earthquake stations closest to the epicentre obtained the mean PGA value as 0.501g. The largest PGA values measured for this earthquake are smaller than the predicted PGA values for both 2007 and 2019.

The lack of damage in reinforced concrete structures using engineering services with regulations from 2007 and later reveals the usefulness of these values in structural calculations. It is clear that damage forming in buildings designed according to the use of the design spectra obtained for DD2, given in the current earthquake regulations and the basis for structural design, will not exceed expected damage levels. According to the obtained PGA values, there is very high earthquake risk in the region and along the EAFZ.

The spectra obtained from the attenuation relationships that used in this study received higher values than the TSDC-2018 predicted for the 72-year return period. The curve proposed in TSDC-2018 is a countable point close to the average curve calculated for the 475 years return period. The spectra for the return period of 2475 years was quite close to the average curve obtained for the attenuation relationships.

Different types of damage occurred in masonry structures built with local material by local construction experts without receiving any engineering services. The low strength of stone walls used in masonry structures formed the basic reason for damage. It is necessary to provide engineering services for masonry structures comprising the majority of construction stock in rural areas. These types of buildings are generally built haphazardly without any seismic design codes and necessary importance given to details. Corner connections of walls should be built well. Deviation from the symmetry of the structural wall patterns should be prevented in the plans and the necessary construction rules should be followed. One of the strategies to reduce damage due to new earthquakes is destruction of very old masonry structures without examining damage status and renewal with projects providing specific optimum design principles for every rural area.

Most damaged RC buildings were determined to have been constructed according to the 1975 earthquake code or previous codes. The general causes of damage formed in RC structures are beams forming plastic hinges due to exceeded carrying strength, buckling of longitudinal reinforcement due to insufficient transverse reinforcement, general use of an older type of smooth reinforcement, lack of use of special earthquake crossties, use of aggregate obtained directly from rivers without any processing, excess segregation in concrete, use of concrete with low resistance, not bending transverse reinforcements by 135°, and insufficient RC (reinforcement and concrete). All these elements are included in the seismic design rules. No damage was observed in structures built according to these rules. The most important cause of damage in carcass structures by the Sivrice (Elazığ) earthquake can be collected under the single main heading of insufficient reinforcement. In this context, it is important to receive the necessary engineering services for application to buildings designed in accordance with seismic design rules. The importance of the strength and dimension concepts for RC structures under the effect of earthquakes was revealed once more.

Turkey, located in an important earthquake zone, has made important gains from significant earthquakes experienced in recent times especially. Beginning in 1940, earthquake-resistant structural design principles have been updated many times over the years and the renewed or full-changed final form entered use in January 2019. The observation of no damage in buildings constructed in accordance with the 2007 and 2019 earthquake codes is a sign that important steps have been taken in terms of earthquake-resistant structural design principles. The clearest example of this may be stated with concrete grade. The minimum concrete grade required for use in the 1975 earthquake code was C14, in 2007 it was C20 and in the final code it is C25. Changes in the 2007 and 2019 regulations make the use of ready-mix concrete mandatory and significantly improve the resistance of structures to earthquakes.

In addition to comparing earthquake parameters with available earthquake data, this study presents information about the EAFZ and is important in terms of revealing the earthquake risk in this fault zone. The cause-effect relationship of damage formed in both masonry and reinforced concrete structures was investigated. This study once again reveals the importance of earthquake-resistant structural design rules.

Acknowledgments

We are grateful to the anonymous reviewers for useful critiques and valuable contributions.

References

Abrahamson, N.A. and Silva, W.J. (1997), "Empirical response spectral attenuation relations for shallow crustal earthquakes", *Seismol. Res. Lett.*, **68**(1), 94-127. https://doi.org/10.1785/gssrl.68.1.94.

ABYYHY (1975), Turkish Earthquake Code, Ministry of Public Works and Settlement, Ankara, Turkey.

Aksoy, E., İnceöz, M. and Koçyiğit, A. (2007), "Lake Hazar Basin: A negative flower structure on the East Anatolian Fault System (EAFS), SE Turkey", *Turkish J. Earth Sci.*, **16**, 319-338.

Ambraseys, N.N., Douglas, J., Sarma, S.K. and Smit, P.M. (2005), "Equations for the estimation of strong ground motions from shallow crustal earthquakes using data from Europe and the Middle East: horizontal peak ground acceleration and spectral acceleration", *B. Earthq. Eng*, **3**(1), 1-53. https://doi.org/10.1007/s10518-005-0183-0.

Anaonymous-2 (2020), "Turkish Earthquake Hazard Map", https://deprem.afad.gov.tr

Anonymous-1 (2020), Press Release-23, https://www.afad.gov.tr.

Anonymous-3 (2020), "Historical Earthquakes", http://www.koeri.boun.edu.tr.

Anonymous-4 (2020), "Historical Earthquakes", https://deprem.afad.gov.tr.

Anonymous-5 (2020), "Sivrice Elazig Earthquake on 24th of January, 2020", http://www.koeri.boun.edu.tr.

Arpat, E. and Saroglu, F. (1972). "The East Anatolian Fault System: thoughts on its development", *Bull. Miner. Res. Explor. Inst.*, **78**, 1-12.

Barka, A.A. and Kadinsky-Cade, K. (1988). "Strike-slip fault geometry in Turkey and its influence on earthquake activity", *Tectonics*, **7(3)**, 663-684. https://doi.org/10.1029/TC007i003p00663.

Bilgin, H. and Huta, E. (2018), "Earthquake performance assessment of low and mid-rise buildings: Emphasis on URM buildings in Albania", *Earthq. Struct.*, **14**(6), 599-614. https://doi.org/10.12989/eas.2018.14.6.000.

Bilgin, H. and Hysenlliu, M. (2020), "Comparison of near and far-fault ground motion effects on low and mid-rise masonry buildings", *J. Build. Eng.*, **30**, 101248. https://doi.org/10.1016/j.jobe.2020.101248.

Biricik, A.S. and Korkmaz, H. (2001), "The seismicity of Kahramanmaraş", *Marmara Coğrafya Dergisi*, **1**(3), 53-82.

Boore, D.M., Joyner, W.B. and Fumal, T.E. (1997), "Equations for estimating horizontal response spectra and peak acceleration from Western North American earthquakes: a summary of recent work", *Seis. Res. Lett.*, **68**(1), 128-153. https://doi.org/10.1785/gssrl.68.1.128.

Calvi, V.S. (1941), *Erdbebenkatalog der Türkei und EinigerBenaehbarterGebiete (unpublished)* (No. 276). MTA Report.

Campbell, K.W. and Bozorgnia, Y. (2003). "Updated near-source ground-motion (attenuation) relations for the horizontal and vertical components of peak ground acceleration and acceleration response spectra", *B. Seismol. Soc. Am.*, **93**(1), 314-331. https://doi.org/10.1785/0120020029.

CC

Çırak, İ.F. (2011). "Damages observed in masonry structures, causes and recommendations". *SDU International Technologic Science*, **3**(2), 55-60.

DBYYHY (2007), Turkish Earthquake Code, Ministry of Public Works and Settlement, Ankara, Turkey.

Duman, T.Y. and Emre, Ö. (2013), "The East Anatolian Fault: geometry segmentation and jog characteristics", *Geol. Soc. London Spec. Publ.*, **372**, 495-529. https://doi.org/10.1144/SP372.14.

Graizer, V. and Kalkan, E. (2007), "Ground motion attenuation model for peak horizontal acceleration from shallow crustal earthquakes", *Earthq. Spectra*, **23**(3), 585-613. https://doi.org/10.1193/1.2755949.

Hadzima-Nyarko, M., Ademović, N., Pavić, G. and Šipoš, T.K. (2018), "Strengthening techniques for masonry structures of cultural heritage according to recent Croatian provisions", *Earthq. Struct.*, **15**(5), 473-485. https://doi.org/10.12989/eas.2018.15.5.473.

Hadzima-Nyarko, M., Morić, D., Pavić, G. and Mišetić, V. (2018), "Spectral functions of damage index (DI) for masonry buildings with flexible floors", *Tehnički Vjesnik*, **25**(1), 181-187. https://doi.org/10.17559/TV-20170516090159.

Haktanır, T. and Elcuman, H. (2007), "*Bingöl ili ve çevresinde kaydedilmiş yıllık ekstrem depremlerin istatistiksel frekans analizi ve yörenin depremselliği, 6. Deprem Mühendisliği Konferansı Bildiriler Kitabı*, 359.

Hempton, M.R. (1981), "The East Anatolian transform fault: along strike variations in geometry and behavior", *EOS Trans.*, **62**, 393.

Idriss, I.M. (2008), "An NGA empirical model for estimating the horizontal spectral values generated by shallow crustal earthquakes", *Earthq. Spectra*, **24**(1), 217-242. https://doi.org/10.1193/070613EQS195M.

Inel, M., Ozmen, H.B. and Akyol, E. (2013), "Observations on the building damages after 19 May 2011 Simav (Turkey) earthquake". *B. Earthq. Eng.*, **11**(1), 255-283. https://doi.org/10.1007/s10518-012-9414-3.

Işık, E. (2016), "Consistency of the rapid assessment method for reinforced concrete buildings", *Earthq. Struct.*, **11**(5), 873-885. http://dx.doi.org/10.12989/eas.2016.11.5.873.

Işık, E. and Özdemir, M. (2017), "Performance based assessment of steel frame structures by different material models", *Int. J. Steel Struct.*, **17**(3), 1021-1031. https://doi.org/10.1007/s13296-017-9013-x.

Işık, E., Işık, M.F. and Bulbul, M.A. (2017), "Web based evaluation of earthquake damages for reinforced concrete buildings", *Earthq. Struct.*, **13**(4), 387-396. https://doi.org/10.12989/eas.2017.13.4.387.

Kabeyasawa, T. (2017), "Damages to RC school buildings and lessons from the 2011 East Japan Earthquake", *B. Earthq. Eng*, **15**(2), 535-553. https://doi.org/10.1007/s10518-015-9825-z.

Karababa, F.S. and Pomonis, A. (2011), "Damage data analysis and vulnerability estimation following the August 14, 2003 Lefkada Island, Greece, earthquake", *B. Earthq. Eng.*, **9**(4), 1015-1046.https://doi.org/10.1007/s10518-010-9231-5.

Karaşin, A. and Öncü, M.E. (2009), "Evaluation of earthquake safety of multi-storey masonry buildings", *Doğu Anadolu Araştırmaları Dergisi*, 63-68.

Karaşin, İ.B., Eren, B. and Işık, E. (2016), "Investigation of an existing masonry building with different rapid assessment method". *Dicle U. Inst. Natural Appl. Sci. J.*, **5**(2), 70-76.

Kartal, R.F., Kadirioğlu, F.T. and Zünbül, S. (2013), "Kinematic of East Anatolian Fault and Dead Sea Fault", *Aktif Tektonik Araştırma Grubu 17. Çalıştayı (ATAG 17*) Antalya.

Köküm, M. and Özçelik, F. (2020), "A case study on reassessment of historical earthquakes: 1789 Palu (Elazığ) earthquake, Eastern Anatolia, Turkey", *Bull. Mineral Res. Explor.*, **161**, 1-10. https://doi.org/10.19111/bulletinofmre.603929.

Korkmaz, A., Çarhoğlu, A.I., Orhon, A.V. and Nuhoğlu, A. (2014), "Effects of different structural material properties on masonry building structural behavior", *Nevşehir J. Sci. Technol.*, **3**(1), 69-78.

Lei, J. and Zhao, D. (2007), "Teleseismic evidence for a break-off subducting slab under Eastern Turkey", *Earth Planet Sc. Lett*, **257**(1-2), 14-28. https://doi.org/10.106/j.epsl.2007.02.011.

McClusky, S., Balassanian, S., Barka, A., Demir, C., Ergintav, S., Georgiev, I., Gurkan, O., Hamburger, M., Hurst, K., Kahle, H., Kastens, K., Kekelidze, G., King, R., Kotzev, V., Lenk, O., Mahmoud, S., Mishin, A., Nadariya, M., Ouzounis, A., Paradissis, D., Peter, Y., Prilepin, M., Reilinger, R., Sanli, I., Seeger, H., Teableb, A., Toksoz, M.N. and Veis, G. (2000), "Global positioning system constraints on plate kinematics and dynamics in the Eastern Mediterranean and Caucasus", *J. Geophys. Res*. **105**, 5695-5719. https://doi.org/10.1029/1999JB900351.

Nalbant, S.S., Mccloskey, J., Steacy, S. and Barka, A.A. (2002), "Stress accumulation and increased seismic risk in Eastern Turkey", *Earth Planet Sci. Lett*., **195**(3-4), 291-298. https://doi.org/10.1016/S0012-821X(01)00592-1.

Özlük, M.H., Işık, E., Günsel, E., Büyüksaraç, A. and Aydın, M.C. (2019). "Investigation of damages on masonry structures in February 2019 Ayvacık Earthquake", 1. *Uluslararası Uygulamalı Bilimler Kongresi,* Diyarbakır, Turkey.

Özlük, M.H., Işık, E., Günsel, E., Büyüksaraç, A. and Aydın, M.C. (2019a), "A case study on the evaluation of damage for masonry structures", *1. Uluslararası Uygulamalı Bilimler Kongresi*, Diyarbakır, Turkey

Pousse-Beltran, L., Nissen, E., Bergman, E.A., Cambaz, M.D., Gaudreau, É., Karasözen, E. and Tan, F. (2020), "The 2020 Mw=6.8 Elazığ (Turkey) earthquake reveals rupture behavior of the East Anatolian Fault", *Geophy. Res. Lett.*, **47**, e2020GL088136, https://doi.org/10.1029/2020GL088136.

Rafi, M.M., Lodi, S.H., Ahmed, M. and Alam, N. (2015), "Observed damages in Pakistan due to 16 April 2013 Iran earthquake", *B. Earthq. Eng.*, **13**(2), 703-724. https://doi.org/10.1007/s10518-014-9638-5.

Sançar, T. and Akyüz, H.S. (2014), "Paleoseismology of the Ilıpınar Segment (Karlıova, Bingöl), the North Anatolian Fault Zone", *Geolog. Bull. Turkey*, **57**(2), 35-52. https://doi.org/10.25288/tjb.298727.

Şaroğlu, F., Emre, Ö. and Kuşçu, I. (1992), "The East Anatolian fault zone of Turkey", *Annales Tectonicae*, 99-125.

Sbeinati, M.R., Darawcheh, R. and Mouty, M. (2005), "The historical earthquakes of Syria: an analysis of large and moderate earthquakes from 1365 BC to 1900 AD", *Annal. Geophys.*, **48(3)**, 347-435. https://doi.org/10.4401/ag-3206.

Šipoš, T.K. and Hadzima-Nyarko, M. (2017), "Rapid seismic risk assessment", *Int. J. Disast. Risk. Re*., **24**, 348-360. https://doi.org/10.1016/j.ijdrr.2017.06.025.

Sunkar, M. (2018), "Major earthquakes and their effects on settlements in Palu (Elaziğ) in the historical and instrumental period", Firat University, Harput Applied and Research Center, International Palu Symposium Proceedings.

Taskin, B. and Tugsal, U.M. (2011), "Analytical investigation of the observed damage in an RC building after March 08, 2010 Kovancilar-Turkey earthquake", *B. Earthq. Eng*, **9**(4), 1047-1065. https://doi.org/10.1007/s10518-010-9237-z.

TSDC (2018), Turkish Seismic Design Code, Ministry of Public Works and Settlement, Ankara, Turke Turkish Earthquake Code (DBYYHY-2007). Ankara, Turkey.

Utkucu, M., Durmus, H., Yalçın, H., Budakoglu, E. and Işık, E. (2013). "Coulomb static stress changes before and after the 23 October 2011 Van, Eastern Turkey, earthquake (Mw=7.1): implications for the earthquake hazard mitigation", *Nat. Hazard Earth Sys*., **13**(7), 1889-1902. https://doi.org/10.5194/nhess-13-1889-2013.

Utkucu, M., Pinar, A. and Alptekin, Ö. (2003), "Investigation of rupture history of the May 22, 1971, Bingöl earthquake obtained from the finite-fault inversion of the teleseismic P waveforms", *Bull. Earth Sci. Appl. Res. Centre of Hacettepe University*, **28**, 65-79.

Yildirim, C. and Kürçer, A. (2007), "Evoluation of Karliova Bingol Earthquake on 26 Ağustos 2007", http://www.mta.gov.tr.

CC